Distribution volumes of macromolecules in human ovarian and endometrial cancers—effects of extracellular matrix structure

Hanne Haslene-Hox,[1] Eystein Oveland,[1] Kathrine Woie,[2] Helga B. Salvesen,[2,3] Olav Tenstad,[1]*
and 🄳 Helge Wiig[1]*

[1]*Department of Biomedicine, University of Bergen, Bergen, Norway;* [2]*Department of Obstetrics and Gynecology, Haukeland University Hospital, Bergen, Norway; and* [3]*Department of Clinical Medicine, University of Bergen, Bergen, Norway*

Haslene-Hox H, Oveland E, Woie K, Salvesen HB, Tenstad O, Wiig H. Distribution volumes of macromolecules in human ovarian and endometrial cancers—effects of extracellular matrix structure. *Am J Physiol Heart Circ Physiol* 308: H18–H28, 2015. First published November 11, 2014; doi:10.1152/ajpheart.00672.2014.—Elements of the extracellular matrix (ECM), notably collagen and glucosaminoglycans, will restrict part of the space available for soluble macromolecules simply because the molecules cannot occupy the same space. This phenomenon may influence macromolecular drug uptake. To study the influence of steric and charge effects of the ECM on the distribution volumes of macromolecules in human healthy and malignant gynecologic tissues we used as probes 15 abundant plasma proteins quantified by high-resolution mass spectrometry. The available distribution volume (V_A) of albumin was increased in ovarian carcinoma compared with healthy ovarian tissue. Furthermore, V_A of plasma proteins between 40 and 190 kDa decreased with size for endometrial carcinoma and healthy ovarian tissue, but was independent of molecular weight for the ovarian carcinomas. An effect of charge on distribution volume was only found in healthy ovaries, which had lower hydration and high collagen content, indicating that a condensed interstitium increases the influence of negative charges. A number of earlier suggested biomarker candidates were detected in increased amounts in malignant tissue, e.g., stathmin and spindlin-1, showing that interstitial fluid, even when unfractionated, can be a valuable source for tissue-specific proteins. We demonstrate that the distribution of abundant plasma proteins in the interstitium can be elucidated by mass spectrometry methods and depends markedly on hydration and ECM structure. Our data can be used in modeling of drug uptake, and give indications on ECM components to be targeted to increase the uptake of macromolecular substances.

ovarian cancer; endometrial cancer; interstitium; extracellular matrix; interstitial fluid; microenvironment; proteomics

THE INTERSTITIUM IS LOCATED between the blood and lymphatic capillary walls and cells in a tissue. It consists of the extracellular matrix (ECM) with collagen fibers as structural elements, a gel-phase of glucosaminoglycans (GAGs), and the interstitial fluid (IF) phase containing ions, proteins, and other solutes. In addition to providing structural features to the interstitium, GAGs and collagen offer significant resistance to interstitial fluid flow (25). Moreover, the structural elements of the ECM will restrict part of the space available and thus exclude soluble macromolecules as proteins from the interstitial space simply because the molecules cannot occupy the same space (51). Tumors often have an increased concentration of collagen and GAGs that can influence the uptake of therapeutic agents (19,

21, 25, 51). Moreover, the physical changes typical for the tumor stroma, such as increased collagen density and matrix stiffness, can promote tumorigenesis and invasion (7). Elucidating the effects of the physical microenvironment on the soluble proteins in the tumor IF can provide important design parameters for therapeutic agents (32).

How the steric and electrostatic exclusion by ECM elements affect the distribution of proteins have been studied in vitro and in vivo in animal tumor models (21) (for review see Ref. 51). Despite the potential clinical importance, data on available and thus excluded volumes in human tumor tissue have to our knowledge not been presented earlier. This may in part be due to the inaccessibility of native IF from human tissue, an issue that can be resolved by using centrifugation for isolation of human tumor interstitial fluid (TIF) (16, 51). Furthermore, high-resolution mass spectrometry (MS) enables quantification of the endogenous abundant plasma proteins present in IF and in tissue eluate by spectral counting (32) that can be used as probes for quantification of the exclusion effect of both normal and malignant human tissues.

We asked whether ECM structural changes observed in experimental animals were reflected in malignant human ovarian tissue. Using plasma proteins as probes we moreover asked whether the tumor ECM excludes macromolecules from a substantial part of the TIF in vivo. We hypothesized that steric exclusion as well as fixed negative charges in the ECM influences the distribution volume of macromolecules, implicating reduced accessibility for macromolecular therapeutic agents. Upon analysis of TIF we found that unfractionated fluid has high concentrations of earlier suggested biomarkers for ovarian and endometrial carcinoma, and may be a valuable substrate for identification of tumor-specific proteins. Surprisingly, we found that the distribution volume of albumin was actually increased in malignant ovarian tissue, most likely due to a reduced amount of collagen and increased hydration compared with that of healthy ovarian tissue. The high tumor tissue hydration was also the likely reason for the modest charge effect on macromolecular distribution volumes. Abundant plasma proteins in unfractionated TIF can accordingly be used to model drug uptake as a function of ECM structure in the tissue.

MATERIAL AND METHODS

Collection of Tissue and Blood Samples from Patients

The research protocol has been approved by the Norwegian Data Inspectorate (Protocol No. 961478-2), Norwegian Social Sciences Data Services (Protocol No. 15501), and the local ethical committee (Protocol ID REKIII nr. 052.01). All samples were collected after obtaining the patients′ written informed consent. The work conformed

---

* O. Tenstad and H. Wiig contributed equally to this article.
Address for reprint requests and other correspondence: H. Wiig, Univ. of Bergen, Dept. of Biomedicine, Jonas Lies vei 91, N-5009 Bergen, Norway (e-mail: helge.wiig@biomed.uib.no).

to the standards set by the latest revision of the Declaration of Helsinki.

Tissue samples of ovarian carcinomas (OC) and endometrial carcinomas (EC) were collected from the Department of Obstetrics and Gynecology at Haukeland University Hospital during surgery. The samples were taken from the tumor surface in an area without any apparent necrosis or inflammation. Tissue from healthy ovaries obtained during surgery of cervical and endometrial cancer without affected ovaries served as healthy ovarian control tissue (OH). Blood samples were collected from the patients 1 to 2 days before surgery, and EDTA was added as the anticoagulation agent before isolation of plasma by centrifugation. The tissue samples were cut in two, and TIF was isolated from one part of the fresh tissue ~60 min after extirpation by centrifugation through a mesh-filter at 106 g for 10 min as described earlier (16, 48). The centrifuged tissue was dried at 60°C for 48 h to determine its water content. TIF was pipetted off avoiding erythrocytes and stored at −80°C until further processing. The second half of tissue was minced into 1–3 mm^3 pieces and incubated with gentle rotation for 48 h at 4°C in a potassium buffer of 0.137 M KCl, 0.05 M H_2KPO_4, and 0.02% potassium azide (pH 7.4) with aprotinin (0.128 TIU/ml) as an antiproteolytic agent. The sample was then centrifuged at 3,220 g for 20 min at 4°C, and the supernatant was pipetted off. The tissue samples and eluate were frozen at −80°C until further analysis.

Albumin Concentration Measured by HPLC

Particles from eluate were removed by filtering samples through 0.22 μm syringe filters. Fifty microliters of filtered eluate was diluted 1:2 in phosphate buffer containing (in M) 0.1 Na_2SO_4, 0.05 HNa_2PO_4, and 0.05 H_2NaPO_4 (pH 6.8), whereas plasma and TIF were diluted 1:336 in phosphate buffer. All samples were analyzed by HPLC using a size-exclusion column (Super SW2000, 4.6 × 300 mm, 18674; Tosoh Bioscience, Tokyo, Japan) and reversed phase column (Proswift Rp4H 1 × 50 mm; Dionex, Sunnyvale, CA) coupled in series. Albumin was separated from IgG and other larger plasma proteins in the first dimension. Subsequently, the sample that eluted in the retention time of albumin was loaded onto the second column by an inline switch at a flow rate of 0.35 ml/min and with an 8-min acetonitrile gradient (5–60%) for separation from proteins with similar molecular weight and quantification of the albumin peak. The albumin concentration was determined based on the area under the curve for standards and samples (16, 48).

Measurement of Na^+

Eluate samples (500 μl) were concentrated using Amicon Ultra-4 Centrifugal Filter Units with 3 kDa cutoff (Millipore, Milford, MA). Na^+ concentration in filtrate and TIF was determined as described previously (16, 48).

Disintegration of Tissue

The tissue from elution was freeze-dried and incubated in digestion buffer (10 mg dried tissue/ml buffer) for 18 h at 65°C. The digestion buffer consisted of 0.150 mg/ml papain (Sigma, St. Louis, MO) in 0.2 M phosphate buffer containing 0.1 M HNa_2PO_4 and 0.1 M H_2NaPO_4 (pH 6.4) with 0.1 M sodium acetate, 0.01 M Na_2EDTA, and 0.005 M cysteine HCl. The samples were centrifuged at 20,000 g for 20 min, and the supernatant was pipetted off and stored at −20°C for further analysis.

Table 1. *Sample overview, with diagnosis, histological subtype, stage, grade, and age at surgery*

Diagnosis and Sample No.	Histological Subtype	Stage	Grade	Age At Surgery
Ovarian cancer				
1	Mucinous borderline tumor	IA	NA	82
2	Papillary serous adenocarcinoma	IIIC	3	69
3	Papillary serous adenocarcinoma	IIIC	3	70
4	Serous adenocarcinoma with low differentiation	IIIC	3	54
5	Clear celled adenocarcinoma	IV	NA	48
6	Papillary serous adenocarcinoma	IV	NA	42
7	Papillary serous adenocarcinoma	IIIC	3	54
8	Serous adenocarcinoma	IIIC	3	66
9	Mucinous borderline tumor	IC	NA	80
10	Papillary serous adenocarcinoma	IIB	3	64
11	Serous adenocarcinoma	IIIC	3	68
12	Papillary serous adenocarcinoma	IIIC	3	85
Endometrial cancer				
13	Undifferentiated carcinoma	IIIC	3	65
14	Adenocarcinoma, endometrioid type, low differentitation	IIIC1	2	67
15	Adenocarcinoma, endometrioid type, low differentitation	IV (4)	3	76
16	Adenocarcinoma, papillary serous type	IB	3	79
17	Adenocarcinoma, endometrioid type, low differentitation	II	3	62
18	Adenocarcinoma, papillary serous type	IB	3	82
19	Adenocarcinoma, partly low differentitation	IIIC2	3	49
20	Adenocarcinoma, endometrioid type, high differentitation	IA	2	83
21	Adenocarcinoma, papillary serous type	IA	3	69
Healthy ovarian tissue				
22	Adenocarcinoma, endometrioid type	IIA	2	75
23	Adenocarcinoma, endometrioid type	IA	1	51
24	Adenocarcinoma, papillary serous type, low differentiation	IB	3	61
25	Hodgins lymphoma			63
26	Serous carcinoma	IIIC2	3	70
27	Adenocarcinoma, papillary serous type	IIIC	3	74
28	Adenocarcinoma, endometrioid type, low differentitation	II	3	62
29	Adenocarcinoma, endometrioid type	II	NA	75

NA, not applicable.

Estimation of Components of the Extracellular Matrix

Collagen content was determined by measuring hydroxyproline according to Woessner (52) as described in a previous publication (48).

Sulfated GAG (sGAG) concentration was measured using the Blyscan sulfated Glycosaminoglycan Assay (BC-B1000; Biocolor, Carrickfergus, U.K.) and hyaluronan (HA) with a hyaluronic acid test kit (Catalog number 029-001; Corgenix, Broomsfield, CO) following instructions provided by manufacturers.

Protein Identification by Mass Spectrometry

The protein concentration in TIF, plasma, and Amicon-filtered eluate was determined by Qubit Quant-IT Protein Assay Kit (Invitrogen, Carlsbad, CA), and ~30 µg of protein from plasma, TIF, and eluate samples were diluted to 30 µl with 100 mM ammonium bicarbonate, digested by trypsin and desalted as described earlier (16, 48).

Iontrap. TIF and eluate samples were analyzed twice in triplicate by liquid chromatography (LC) coupled to tandem mass spectrometry (MS/MS) on an Agilent 1100 LC/MSD Trap XCT Plus system with a HPLC-Chip/MS interface. The HPLC-Chip contained a 0.075×43 mm ZORBAX 300SB C18 5-µm column and an integrated 9 mm 160 nl enrichment column packed with the same material (part no. G4240-63001 SPQ110; Agilent Technologies).

Label-free analysis of individual samples with LTQ orbitrap velos pro. Digested TIF samples were analyzed using an LTQ Orbitrap Velos Pro mass spectrometer (Thermo Scientific, Waltham, MA) as described earlier (17).

The software Progenesis LC-MS (Nonlinear Dynamics, Newcastle, UK) was used for label-free quantification and comparison of LC-MS Orbitrap data as previously detailed (17).

Calculation of Protein Distribution Volumes

To assess the distribution volumes of a larger number of proteins with a span of molecular size and charge, we used the spectral data from the most abundant plasma proteins detected in native IF after MS-analysis. The extracellular distribution volume V_A for protein x, V_{Ax}, was calculated as $V_{Ax} = [(E_X/S_X) \div (E_{Alb}/S_{Alb})] \cdot V_{Alb}$, where S is the number of spectra detected in IF, E is the number of spectra detected in eluate, and V_{Alb} is the distribution volume for albumin.

Statistical Analysis

SPSS (IBM SPSS Statistics, version 19.0.0.2; IBM, Armonk, NY) and Graphpad Prism (Software version 5.0; Graphpad Software, La Jolla, CA) were used for statistical analysis, and data were compared using nonparametric Mann-Whitney tests unless otherwise specified. A P value of <0.05 was considered statistically significant. All values are presented as means ± SE.

RESULTS

The mean age of all patients included in this study was 67.1 ± 11.4 years, and there was no statistical difference between the ages of the patients at surgery in different groups. An overview of the samples used with age, diagnosis, and histological subtype is given in Table 1.

Fluid Volumes

Hydration. We first measured water content since this parameter is an important determinant of the space accessible to proteins (51). Median water content was slightly elevated in OC ($P = 0.011$) and EC ($P = 0.016$) compared with OH (Fig. 1A and Table 2), whereas the water content in EC and OC did not differ significantly. Three samples in OC had a marked higher hydration than the other samples in the OC group, the
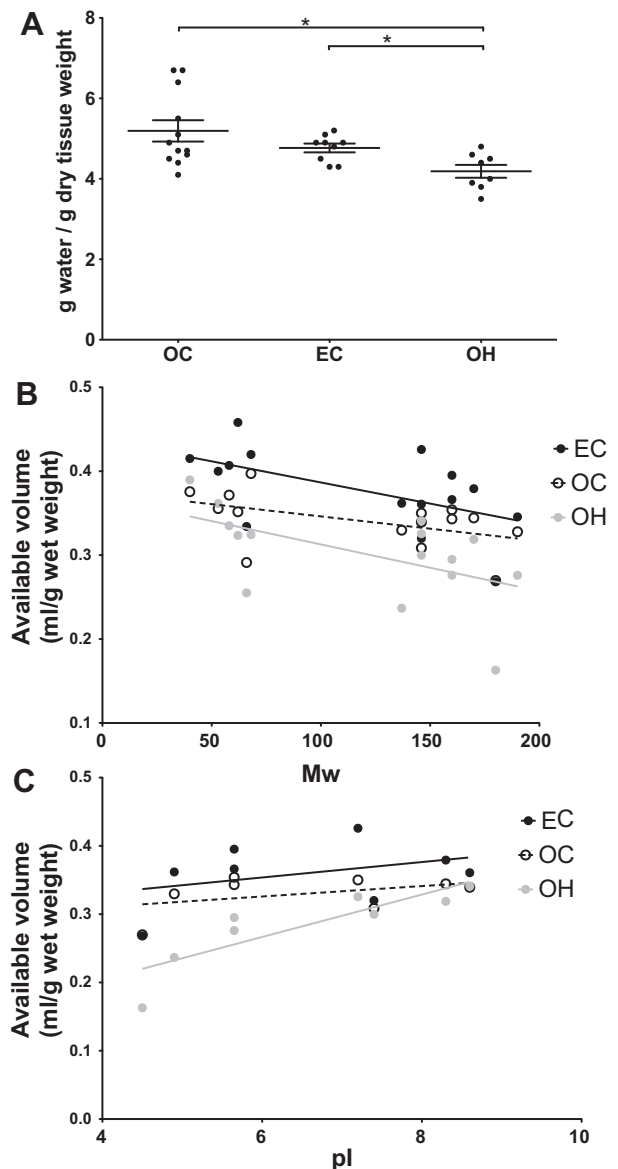
Fig. 1. *A*: hydration of samples of ovarian carcinoma (OC; $n = 12$), endometrial cancer (EC; $n = 9$), and healthy ovarian tissue (OH; $n = 8$). *$P < 0.05$, Mann-Whitney test. *B*: available volume for 15 abundant plasma proteins as a function of molecular weight for OC, EC, and OH. The points represent the mean of the available volume for a given protein in all patients within each group. Linear regression lines for OC (y = $-2.92 \cdot 10^{-4}$x + 0.38; $R^2 = 0.011$; $P = 0.16$), EC (y = $5.04 \cdot 10^{-4}$x + 0.44; $R^2 = 0.03$; $P = 0.04$), and OH (y = $-5.6 \cdot 10^{-4}$x + 0.37; $R^2 = 0.07$; $P = 0.004$) are given. *C*: available volume of 15 abundant plasma proteins as a function of pI for OC, EC, and OH. The points represent the mean of the available volume for a given protein in all patients within each group. Linear regression lines for OC (y = 0.0076x + 0.28; $R^2 = 0.006$; $P = 0.44$), EC (y = 0.011x + 0.29; $R^2 = 0.014$; $P = 0.32$), and OH (y = 0.03x + 0.08; $R^2 = 0.18$; $P = 0.0006$) are given.

two mucinous carcinomas (samples 1 and 9), and a serous ovarian carcinoma (sample 7).

Total extracellular volume. Because Na^+ is found predominantly in the extracellular fluid, we can calculate the total extracellular volume (ECV) in the tissue samples by using the concentration of Na^+ in eluate, yielding total mass of Na^+, and in IF, yielding the extracellular concentration. A requirement is that the isolated sample is of extracellular origin, as can be assessed by the

Table 2. *Hydration, interstitial fluid protein concentration, collagen, sulphated glucosaminoglycans, and hyaluronan for OC, EC, and OH*

	Hydration, g water/g dw	Protein, mg/ml	Collagen, mg/g dw	Sulphated Glucosaminoglycans, mg/g dw	Hyaluronan, mg/g dw
OC	5.19 ± 0.27	42.8 ± 3.3	182.3 ± 32.4	25.0 ± 3.5	0.479 ± 0.097
EC	4.77 ± 0.11	42.9 ± 3.2	71.43 ± 19.2	22.9 ± 3.9	0.469 ± 0.077
OH	4.19 ± 0.16	50.9 ± 5.3	342.1 ± 30.7	26.2 ± 3.8	0.041 ± 0.008

Values are means ± SE.

Na^+-ratio between IF and plasma (16). The Na^+-ratios for OC and OH were both 0.8 ± 0.3, not significantly different from 1.0, whereas the ratio for EC, 0.5 ± 0.2, was significantly lower than 1.0 ($P < 0.05$, Wilcoxon signed rank test), indicating admixture of intracellular fluid and possibly also a higher cellularity in EC. Such admixture precluded the use of Na^+ concentration to calculate ECV in EC, and therefore ECV was calculated in OC and OH only. The Na^+-space, and thus extracellular volume of OC and OH, was 0.49 ± 0.05 and 0.53 ± 0.05 ml/g wet weight (ww), concurrent with earlier determinations of ECV in experimental animal tumors (27, 51).

Distribution volume of albumin. The matrix elements of the interstitium will limit the space available for macromolecules from a fraction of the interstitial fluid. In analogy with the estimation of total ECV using Na^+ above, we calculated the available volume for albumin using the albumin concentrations in IF and the corresponding mass calculated from eluate concentration. Thus the albumin distribution volume was 0.33 ± 0.04 and 0.26 ± 0.02 ml/g ww for OC and OH, respectively, or 67% and 49% of the extracellular volume. Although the absolute distribution volumes for albumin were not different between OC and OH, the fractional available volume was significantly higher in OC compared with OH ($P = 0.04$).

Distribution volume of abundant plasma proteins assessed by MS. We then asked whether the distribution volume, V_A, was dependent on molecular weight or charge in healthy or malignant gynecologic tissue. To this end we determined V_A for 15 known abundant plasma proteins that were detected by more than three spectra in both IF and eluate in all patients (Table 3), and included proteins with molecular weights rang-

ing from 40 to 190 kDa, and pI from 1.8 to 8.6. The concentration of soluble proteins in isolated IF was not significantly different for OC, EC, and OH (Table 2), averaging 45.1 ± 12.2 mg/ml across all samples.

To determine whether V_A is dependent on molecular size, we expressed V_A as a function of molecular weight for all 15 plasma proteins used as probes (Fig. 1*B*). The distribution volumes in EC and OH were decreasing with increased molecular weight (linear regression, $P = 0.033$ and $P = 0.003$, respectively), whereas this relationship was not significant in OC ($P = 0.16$). Of note, IgG (146 kDa), previously used as probe in rat tumors (49), had V_A of 0.34 ± 0.02 ml/g in OC and 0.32 ± 0.02 ml/g in OH, not different from that of albumin ($P = 0.23$ and $P = 0.12$ for OC and OH, respectively). Furthermore, the dependence of V_A as a function of pI, and thereby of protein charge, was regarded using all proteins, as well as by grouping the proteins according to molecular weight. The distribution volume did not show correlation with pI when considering the entire molecular weight range, nor in the low molecular weight area (57–77 kDa, results not shown). In the high molecular weight range (137–180 kDa) the distribution volume in OH increased for proteins with increasing pI (Fig. 1*C*); thus proteins with a more positive charge at physiologic pH had an increased distribution volume compared with negatively charged proteins of similar size in OH.

ECM Components

Tumor tissue can have a heterogeneous ECM composition that may affect macromolecular distribution volume (25). We

Table 3. *Selected plasma proteins used as probes for determination of available volume, with Uniprot accession numbers, names, molecular weight, pI, and available distribution volume*

Accession No.	Name	Molecular Weight, kDa	pI	Available Distribution Volume		
				OC	EC	OH
P02763	α-1-Acid glycoprotein 1	40 (26)	1.8 (23)	0.44 ± 0.08	0.42 ± 0.04	0.39 ± 0.04
P01011	α-1-Antichymotrypsin	68 (44)	3.9 (39)	0.48 ± 0.10	0.42 ± 0.07	0.32 ± 0.03
P01009	α-1-Antitrypsin	53 (31)	4.5 (23)	0.43 ± 0.09	0.40 ± 0.04	0.36 ± 0.04
P01023	α-2-Macroglobulin	180 (40)	4.5 (36)	0.32 ± 0.08	0.27 ± 0.03	0.16 ± 0.03
P00450	Ceruloplasmin	137 (5)	4.9 (5)	0.40 ± 0.09	0.36 ± 0.05	0.24 ± 0.03
P01024	Complement C3	190 (6)	5.9 (2)	0.39 ± 0.09	0.35 ± 0.04	0.28 ± 0.05
P02790	Hemopexin	62 (3)	5.7 (3)	0.41 ± 0.07	0.46 ± 0.06	0.32 ± 0.04
P01876	Ig α-1 chain C region	160 (20)	5.7 (24)	0.39 ± 0.06	0.37 ± 0.05	0.30 ± 0.04
P01877	Ig α-2 chain C region	160 (20)	5.7 (24)	0.39 ± 0.06	0.40 ± 0.08	0.28 ± 0.03
P01857	Ig γ-1 chain C region	146 (15)	8.6 (15)	0.39 ± 0.06	0.36 ± 0.04	0.34 ± 0.04
P01859	Ig γ-2 chain C region	146 (15)	7.4 (15)	0.36 ± 0.07	0.32 ± 0.03	0.30 ± 0.04
P01860	Ig γ-3 chain C region	170 (15)	8.3 (15)	0.40 ± 0.07	0.38 ± 0.04	0.32 ± 0.05
P01861	Ig γ-4 chain C region	146 (15)	7.2 (15)	0.40 ± 0.05	0.43 ± 0.04	0.33 ± 0.03
P02768	Serum albumin	66 (26)	5.2 (23)	0.34 ± 0.06	0.33 ± 0.05	0.26 ± 0.02
P02774	Vitamin D-binding protein	58 (41)	4.9 (41)	0.44 ± 0.08	0.41 ± 0.05	0.34 ± 0.04

Values are means ± SE.

therefore estimated the concentrations of the extracellular components collagen, HA, and sGAGs in all excised tissue samples used for determination of V_A (Table 2).

Collagen. The collagen contents of both ovarian ($P = 0.0087$) and endometrial ($P = 0.00053$) carcinomas were significantly lower than that in the healthy ovarian tissue (Table 2 and Fig. 2*A*). Negligible amounts of collagen were detected in eluates.
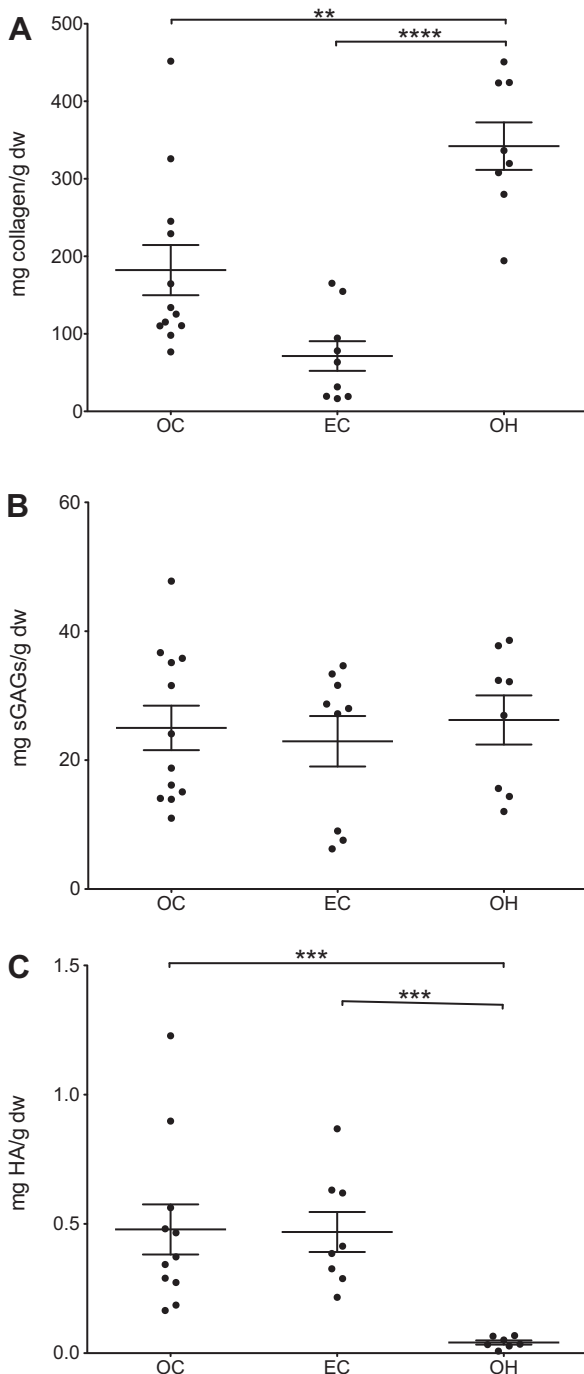
Fig. 2. Extracellular matrix components in OC, EC, and OH expressed as dry tissue weight (dw). *A*: collagen content ($n_{OC} = 12$, $n_{EC} = 9$, $n_{OH} = 8$). **$P < 0.01$; ****$P < 0.0001$, Mann-Whitney test. *B*: sulphated glucosaminoglycans (sGAG; $n_{OC} = 12$, $n_{EC} = 9$, $n_{OH} = 8$). *C*: hyaluronan (HA; $n_{OC} = 11$, $n_{EC} = 8$, $n_{OH} = 7$). ***$P < 0.001$, Mann-Whitney test.

sGAGs. The concentrations of sGAGs in the tissue were not significantly different in OC, EC, and OH (Fig. 2*B* and Table 2), with eluates containing negligible amounts of sGAGs.

The IF samples were also analyzed by MS, and 10 proteoglycan proteins were detected in the material: Versican core protein (P13611); Aggrecan core protein (P16112); Lumican (P51884); Fibromodulin (Q06828); Dystroglycan (Q14118); Basement membrane-specific heparan sulfate proteoglycan core protein (P98160); Hyaluronan and proteoglycan link protein 2 (Q9GZV7); Proteoglycan 4 (Q92954); Agrin (O00468) and Decorin (P07585), of which four were significantly upregulated in OC compared with OH (Versican core protein, Lumican, Aggrecan core protein and Fibromodulin, $P < 0.05$, Kolmogorov-Smirnov test). Summarizing the normalized abundance for all 10 proteins, the difference between OC and OH remained significant ($P = 0.003$).

Hyaluronan. Because repeated elution and subsequent centrifugation can release up to 40% of the tissue HA in solution (1), we analyzed the eluate for HA. We found that ~20% of the HA originating from the tissue could be found in the tissue eluate of OC and OH, whereas significantly more HA in EC tissue was released during elution (60%) compared with both OH and OC. Analysis of HA in tissue and eluate (Fig. 2*C* and Table 2) showed that the HA concentration of OC ($P = 0.0049$) and EC ($P = 0.0055$) was significantly higher than for OH.

MS analysis showed that CD44 antigen (P16070) was upregulated in EC compared with OH (Kolmogorov-Smirnov test, $P = 0.02$), and Inter-α-trypsin inhibitor heavy chain H3 (Q06033), which can act as a binding protein for HA and other matrix proteins in tissue, was upregulated in both EC ($P = 0.02$) and OC ($P = 0.05$) compared with OH.

IF Proteome

We used a MS-based strategy to quantify multiple abundant plasma proteins with different size and charge as probes to address the question of how these factors affect their distribution volume in the tissue microenvironment. A positive side effect of this approach was the quantification of other proteins that may give functional information about the biological processes in the tissue. The medium-to-high abundance proteomes of IF, eluate, and plasma yielded 1,590, 1,864, and 381 proteins that were identified in one or more of the IF, eluate, and plasma samples, respectively (Fig. 3). Of all the proteins detected in one or more of the proteomes, 45%, 48%, and 70% were found in all three groups for IF, eluate, and plasma, respectively. EC had the most proteins only detected in one proteome in IF and eluate (22% and 16%), probably reflecting the increased cell lysis indicated by the low Na^+-ratio, whereas OC had the largest number of unique proteins in plasma (11%).

The much larger number of proteins in IF compared with plasma underlines the advantage of using IF over plasma as a starting point for biomarker discovery, and we assessed the potential of this approach for biomarker discovery by a brief analysis of a few proposed biomarker candidates.

Tumor-specific proteins. To assess the potential of the identified proteomes as a source for biomarker candidates, we selected the 587 proteins with a *P* value less than 0.05 when comparing EC with OH, OC with OH, or EC with OC, judged by the Kolmogorov-Smirnov test, and compared these proteins
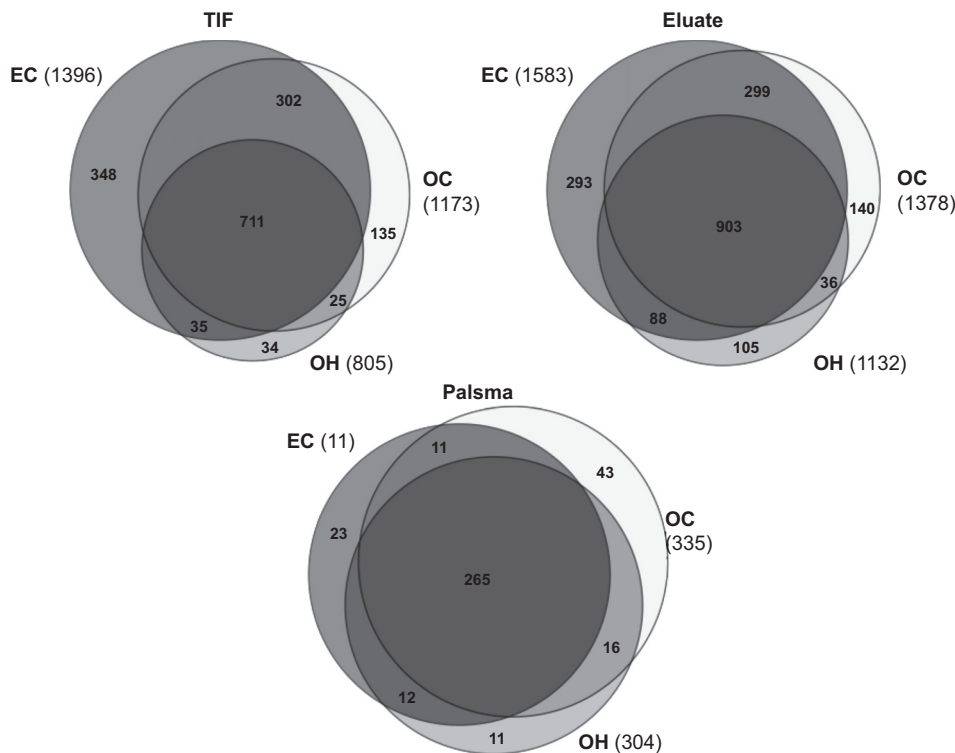
Fig. 3. Venn-diagrams of the proteins identified with spectra in interstitial fluid (IF), eluate and plasma in OC, EC, and OH samples. Number of proteins identified is given for each section. TIF, tumor IF.

to the list of known biomarkers compiled by Polanski and Anderson (33). From our data set, 81 proteins, or 14% (Table 4), were corresponding to those reviewed by Polanski and Anderson (33). Of these, we looked closer at three proteins. Stathmin (P16949) was upregulated in EC compared with OH (Fig. 4A; $P = 0.012$), and the S100 calcium binding proteins A8 (P05109) and A9 (P06702) were found in significantly higher amounts in EC compared with both OH ($P = 0.012$; Fig. 4B) and OC ($P = 0.004$; KS). Two related proteins, S100A4 and S100A13, were upregulated in OC compared with OH (data not shown).

In addition to the proteins that are common to the biomarker list compiled by Polanski and Anderson in 2007 (33), many proteins have been suggested as biomarkers since then, and we highlight four additional proteins that may be relevant for ovarian or endometrial cancer. Stress-induced phosphoprotein 1 (STIP1, P31948) was upregulated in both OC ($P = 0.028$) and EC ($P = 0.012$) compared with OH (Fig. 4C). Histidine-rich glycoprotein (HRG, P04196) was expressed in significantly higher amounts in OC compared with EC ($P = 0.01$), with the same tendency between OC and OH, with borderline significance ($P = 0.07$; Fig. 4D). Spindlin-1 (Q9Y657), also called ovarian cancer-related protein, was significantly increased in OC compared with OH (Fig. 4E; $P = 0.009$). Programmed cell death 6-interacting protein (PCD6I, Q8WUM4; Fig. 4F) was identified with low expression in OH, whereas the expression in both EC ($P = 0.002$) and OC ($P = 0.003$) were significantly upregulated. By analyzing native samples of TIF from individual patients, we are able to detect several proteins that have earlier been suggested as biomarkers, and show that the abundance of tumor-specific proteins are sufficient for detection by a high-resolution mass spectrometer such as the Orbitrap.

DISCUSSION

To our knowledge, data on directly measured extracellular and protein available volume have never been reported in human tumors. Here we determined the extracellular volume using Na^+ as an internal tracer and label-free quantitative proteomics to identify and quantify abundant plasma proteins applied as endogenous probes. We could thereby assess protein available and excluded volume as a function of size and charge, and demonstrated a size-dependent exclusion of abundant plasma proteins between 40 and 190 kDa, as well as charge-dependent exclusion of high molecular weight proteins, in healthy ovarian tissue, but not in ovarian carcinoma. Serum albumin distributed in 67% of the extracellular space in OC, exceeding that of normal ovarium. These data are important when considering the concentrations of macromolecular therapeutic agents in the tumor microenvironment, as well as in designing novel treatments for ovarian and endometrial cancer.

Methodological considerations—limitations of the study. To measure available volume in the interstitium we need to estimate interstitial mass of the respective protein and its concentration in the interstitial fluid. Although we have evaluated the TIF isolation method thoroughly in an animal tumor model (48) and in human ovarian cancers (16), and shown that the elution method gives complete protein recovery from skin (37), the fact that we studied human tumors results in additional questions and poses limitations. One such question is the ~60-min period needed from tissue extirpation until TIF harvesting. During this period metabolic processes may result in tissue degradation and cell lysis and thereby contamination of TIF with intracellular proteins. Based on analyses of the mostly extracellular ion Na^+, there are no indications that cell lysis is a problem (16). Immediate freezing of the tissue and subse-

Table 4. *Proteins identified as differentially regulated between OC and OH, EC and OH, and/or EC and OC (P < 0.05) in our data set also present in the list of cancer biomarkers published by Polanski and Anderson (33)*

Entry	Entry Name	Protein Name
Q04917	1433F_HUMAN	14-3-3 protein eta
P01011	AACT_HUMAN	α-1-Antichymotrypsin
P42684	ABL2_HUMAN	Abelson tyrosine-protein kinase 2
P53396	ACLY_HUMAN	ATP-citrate synthase
P09972	ALDOC_HUMAN	Fructose-bisphosphate aldolase C
P04083	ANXA1_HUMAN	Annexin A1
P07355	ANXA2_HUMAN	Annexin A2
P63010	AP2B1_HUMAN	AP-2 complex subunit β
P02649	APOE_HUMAN	Apolipoprotein E
P04040	CATA_HUMAN	Catalase
P08571	CD14_HUMAN	Monocyte differentiation antigen CD14
P16070	CD44_HUMAN	CD44 antigen
P21926	CD9_HUMAN	CD9 antigen
Q16543	CDC37_HUMAN	Hsp90 co-chaperone Cdc37
P00450	CERU_HUMAN	Ceruloplasmin
O00299	CLIC1_HUMAN	Chloride intracellular channel protein 1
P13671	CO6_HUMAN	Complement component C6
P10643	CO7_HUMAN	Complement component C7
P04080	CYTB_HUMAN	Cystatin-B
P06733	ENOA_HUMAN	α-Enolase
P15311	EZRI_HUMAN	Ezrin
Q01469	FABP5_HUMAN	Fatty acid-binding protein, epidermal
P49327	FAS_HUMAN	Fatty acid synthase
P39748	FEN1_HUMAN	Flap endonuclease 1
P02751	FINC_HUMAN	Fibronectin
P02794	FRIH_HUMAN	Ferritin heavy chain
P02792	FRIL_HUMAN	Ferritin light chain
Q16658	FSCN1_HUMAN	Fascin
P07900	HS90A_HUMAN	Heat shock protein HSP 90-α
P34932	HSP74_HUMAN	Heat shock 70 kDa protein 4
Q15056	IF4H_HUMAN	Eukaryotic translation initiation factor 4H
Q12906	ILF3_HUMAN	Interleukin enhancer-binding factor 3
Q14624	ITIH4_HUMAN	Inter-α-trypsin inhibitor heavy chain H4
P08727	K1C19_HUMAN	Keratin, type I cytoskeletal 19
P05787	K2C8_HUMAN	Keratin, type II cytoskeletal 8
P12277	KCRB_HUMAN	Creatine kinase B-type
P07942	LAMB1_HUMAN	Laminin subunit β-1
P00338	LDHA_HUMAN	L-lactate dehydrogenase A chain
P56470	LEG4_HUMAN	Galectin-4
P27361	MK03_HUMAN	Mitogen-activated protein kinase 3
Q16539	MK14_HUMAN	Mitogen-activated protein kinase 14
P36507	MP2K2_HUMAN	Dual specificity mitogen-activated protein kinase kinase 2
P43490	NAMPT_HUMAN	Nicotinamide phosphoribosyltransferase
P13591	NCAM1_HUMAN	Neural cell adhesion molecule 1
Q92597	NDRG1_HUMAN	Protein NDRG1
P36955	PEDF_HUMAN	Pigment epithelium-derived factor
P05164	PERM_HUMAN	Myeloperoxidase
Q13526	PIN1_HUMAN	Peptidyl-prolyl *cis*-trans isomerase NIMA-interacting 1
P14923	PLAK_HUMAN	Junction plakoglobin
P00747	PLMN_HUMAN	Plasminogen
P09086	PO2F2_HUMAN	POU domain, class 2, transcription factor 2
P27169	PON1_HUMAN	Serum paraoxonase/arylesterase 1
P32119	PRDX2_HUMAN	Peroxiredoxin-2
Q13162	PRDX4_HUMAN	Peroxiredoxin-4
P20742	PZP_HUMAN	Pregnancy zone protein
Q09028	RBBP4_HUMAN	Histone-binding protein RBBP4
P54725	RD23A_HUMAN	UV excision repair protein RAD23 homolog A
P54727	RD23B_HUMAN	UV excision repair protein RAD23 homolog B
P08134	RHOC_HUMAN	Rho-related GTP-binding protein RhoC
P29034	S10A2_HUMAN	Protein S100-A2
P26447	S10A4_HUMAN	Protein S100-A4

Continued

Table 4.—*Continued*

Entry	Entry Name	Protein Name
P31151	S10A7_HUMAN	Protein S100-A7
P05109	S10A8_HUMAN	Protein S100-A8
P06702	S10A9_HUMAN	Protein S100-A9
Q15019	SEPT2_HUMAN	Septin-2
P04179	SODM_HUMAN	Superoxide dismutase [Mn], mitochondrial
P16949	STMN1_HUMAN	Stathmin
Q03403	TFF2_HUMAN	Trefoil factor 2
P01033	TIMP1_HUMAN	Metalloproteinase inhibitor 1
P02788	TRFL_HUMAN	Lactotransferrin
Q16881	TRXR1_HUMAN	Thioredoxin reductase 1, cytoplasmic
P02766	TTHY_HUMAN	Transthyretin
P19971	TYPH_HUMAN	Thymidine phosphorylase
P22314	UBA1_HUMAN	Ubiquitin-like modifier-activating enzyme 1
P17948	VGFR1_HUMAN	Vascular endothelial growth factor receptor 1
P09327	VILI_HUMAN	Villin-1
P04004	VTNC_HUMAN	Vitronectin
Q14508	WFDC2_HUMAN	WAP 4-disulfide core domain protein 2
P13010	XRCC5_HUMAN	X-ray repair cross-complementing protein 5
P12956	XRCC6_HUMAN	X-ray repair cross-complementing protein 6
P25311	ZA2G_HUMAN	Zinc-α-2-glycoprotein

quent fluid isolation would stop metabolism, but results in cell lysis and dilution of TIF (16) and is therefore not an alternative. Another challenge is that the tumor vascular structure is highly variable, contributing inter alia to a high interstitial fluid pressure (11) that may affect extracellular volume, hydration, and composition. We tried to minimize this effect by harvesting from the tumor surface in a standardized way from an area without any apparent necrosis or inflammation, but are aware that this may not be sufficient to completely compensate for this problem. Moreover, the intra- and extravascular protein composition may differ and result in a different concentration in native extravascular fluid and TIF, but such influence should be minimal due to a low extravascular volume fraction in tumors (48).

We used EC as an alternative tumor to OC to evaluate another tumor type and acknowledge that OH may not be a representative control for the former. Normal endometrium might have served as control for EC, but the endometrium in postmenopausal women is very thin and not suitable for TIF isolation by centrifugation. Moreover, if such tissue could be obtained it might not represent healthy tissue since patients treated for cancer in other sites in the gynecological tract (as ovarian cancer) are usually more advanced and often include growth into the uterus.

Because of a potential charge effect we decided to evaluate the tumor distribution volume of differentially charged probes. Because of limited sample volume we could not evaluate the pI of the applied probes as in a recent publication in rats (37) but had to use published values that may deviate from the actual ones. Most of the plasma proteins used as probes have a negative charge at normal pH and thus are less ionized in tumors because of the inherent lower pH in tumors (51). Accordingly, the charge effect on distribution volume, shown to be substantial in skin in vitro (50) and in vivo (14), may be underestimated by our present approach.

Relevance of data in relation to previous studies. We performed these experiments based on the hypothesis that ECM composition would affect macromolecular distribution and
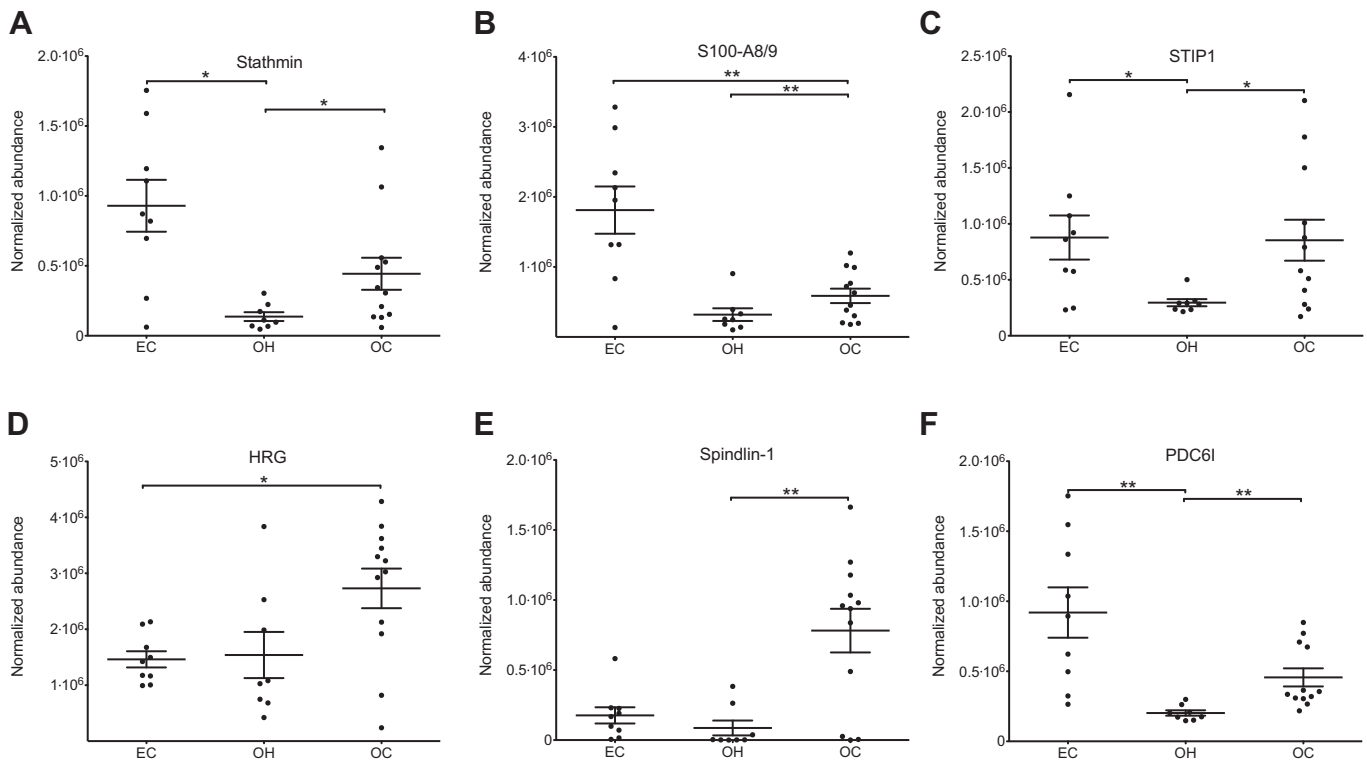
Fig. 4. *A–F*: selected cancer-related proteins as quantified by normalized abundance in the Progenesis software for EC ($n = 9$), OH ($n = 8$), and OC ($n = 12$). Significant differences (Kolmogorov-Smirnov test) are annotated. $*P < 0.05$; $**P < 0.01$.

thereby tissue uptake, and further assessed the ECM composition in all three tissues to evaluate the contribution of ECM components to protein exclusion. As also demonstrated here, healthy ovarian tissue has a rather high concentration of collagen (34), exceeding that in ovarian carcinoma. Interestingly, the concentration in human ovarian carcinomas is markedly higher than in ovarian tumor xenografts (8) as well as other animal tumor models (Table 3 in Ref. 51). Thus, human tumor samples may have a substantially higher collagen content than tumors from animal models, underlining the importance of assessing ECM composition in clinical samples. For HA, however, the concentrations found in both EC and OC were comparable with that of ovarian tumor xenografts in mice (8). These data were also consistent with earlier reports on an increase of HA in ovarian carcinomas relative to healthy ovarian tissue (18, 29) and endometrial carcinoma (29).

We had expected that the dense ECM in tumors (19, 25) and marked increase in negatively charged matrix components (43) would have resulted in a reduced distribution volume of the negatively charged albumin molecule, whereas the opposite was actually observed. Moreover, in contrast with findings in rat skin (49), we found that pI only affected V_A in OH, the tissue with the lowest hydration, and only for proteins with molecular weight exceeding 138 kDa. Part of the explanation for the increased V_A in OC can be a much lower absolute content of GAGs in ovarian tissue; another factor can be reduced ionization of acidic plasma proteins due to a lower pH in the tumor interstitium (51) as discussed above. However, the most important factor is likely the difference in hydration in the two tissues. Notably, the hydration measured in the human tissue is much higher than that observed in rat models (51). By

summarizing data from several studies we showed that there is a strong relationship between V_A and hydration (51). Such increased hydration will result in increased distances between both solid, neutral (notably collagen) and negatively charged tissue elements in the ECM and thus result in reduced exclusion due to steric as well as charge effects, explaining the observed lack of correlation between molecular weight and distribution volume. These assumptions are supported by mathematical modeling experiments (28), and moreover by our finding of size and charge effects on distribution volume in the less hydrated OH. In line with this and with findings in rat tumors (49), we found similar V_A for albumin and IgG in OC and OH. Whereas we have previously interpreted this observation to be a consequence of negative repulsive forces increasing the apparent size of albumin, it here appears to be resulting from lack of size sensitivity on V_A in tissues with high hydration.

Others have studied the relationship between macromolecular size and distribution volume. Krol et al. (21) found that V_A in tumor tissue decreased abruptly with probe sizes above 40 kDa, whereas the decrease in V_A between 70 and 2,000 kDa was modest. The fact that all the plasma proteins used as probes here had molecular weights >40 kDa may explain the small reduction in V_A with increasing molecular weight, concurrent with previous findings (21).

EC had a higher V_A than OH in the entire molecular weight range, but the reduction in V_A at increasing molecular weight was similar to OH. Although the hydration of EC was somewhat higher than for OH, the size-dependent exclusion was evident for EC. However, the hydration of EC and OC was not

significantly different, and the effect on V_A can likely not be explained solely by hydration.

Using a previous applied approach (49), we can estimate the exclusion effect for albumin caused by the individual ECM components and thereby interpret our data in the context of interstitial structure. We found an excluded volume of 33%, or 0.16 ml/g ww for OC and 51% or 0.27 ml/g ww for OH. Highly organized collagen will exclude albumin from 1.6 ml/g (4), whereas HA will contribute with 0.05 ml/mg (22), and sGAGs with 0.044 ml/mg (49). Using these numbers and our ECM structure data, we arrive at calculated theoretical albumin exclusion values of 0.24 and 0.33 ml/g ww for OC and OH, respectively, and thus a contribution of collagen, HA, and sGAGs of 20%, 2%, and 78% for OC, and 32%, 1%, and 67% for OH. The theoretical values are close to the measured, and the slight increase can be due to the differences in organization of the ECM components in vitro and in vivo. According to these estimates, the sGAGs are the major contributors to exclusion, whereas the difference in collagen content is the main cause for the discrepancy in albumin distribution volumes in OC and OH. Important to note, the large sGAGs will contribute substantial steric in addition to electrostatic exclusion. Taken together, such calculations give indications on which ECM component to be targeted to increase tissue uptake of macromolecular substances.

Relevance of data for biomarker studies. Although merely a distribution effect, the observed difference in available volume in healthy and cancer tissue might appear as a difference in protein expression. This should be borne in mind in biomarker discovery studies that use tissue samples, where proteins such as serum albumin, ceruloplasmin, and α-2-macroglobulin have been interpreted to be differentially expressed (46). Such abundant plasma proteins are, however, mainly present in the tissue due to bulk flow and diffusion from blood, and the apparent difference in expression can be caused by variable ECM structure and protein distribution volume between patient groups. This is because a larger available volume will result in an increased total amount, but not in vivo concentration of a protein. Thus, when tissue samples are used for biomarker discovery, especially in the case of whole tissue, care should be taken to choose biomarker candidates that are likely locally produced.

Although our major aim was to use a proteomic approach to quantify several abundant macromolecular probes to be used, this approach also resulted in the identification of many proteins of interest in a biomarker context as might be expected using TIF as a substrate (12). Several earlier reported biomarker candidates were here found to be increased in OC and EC compared with OH, such as stathmin (45), several members of the S100 calcium binding protein group (9, 13, 38), STIP1 (47), spindlin-1 (10), and PCD6I (30, 42). Indeed, some were verified in clinical samples on protein level for the first time. Also, in contrast with earlier reports of reduced HRG in tumor tissue (35), we actually found that HRG was higher in OC, which may be explained by the presence of HRG as a not actively regulated plasma protein that is affected by the size-dependent exclusion of OH and EC.

The proteins mentioned are only a few examples of possibly cancer-related proteins that were found regulated in this data set, and additional validation will have to be performed to verify if any of the mentioned proteins, or other proteins in the

data set have biomarker potential. However, the full in-depth proteomic analysis is considered beyond the scope of this article.

To summarize, we here show that abundant plasma proteins, which are detected with a high number of spectra in native IF, can be used to determine barrier properties of the tumor microenvironment, e.g., the accessibility for therapeutic agents in tumor tissue. We found that the distribution volume of macromolecules between 40 and 190 kDa decreased with size for endometrial carcinoma and healthy ovarium, but was independent of molecular weight for the well-hydrated ovarian carcinoma. Furthermore, there was only effect of charge on macromolecular distribution volume at low hydration and high collagen content, indicating that a condensed interstitium increase the influence of the negative charges. We moreover found that interstitial fluid can be a valuable source for tissue-specific proteins in the search for novel biomarker candidates. Our data suggest that the highly abundant part of the tumor interstitial fluid proteome may contain reliable and clinically important data on the tumor microenvironment and tissue structure, and give indications on which ECM component to be targeted to increase uptake of macromolecular substances.

DISCLOSURES

No conflicts of interest, financial or otherwise, are declared by the author(s).

AUTHOR CONTRIBUTIONS

Author contributions: H.H.-H., E.O., K.W., and O.T. performed experiments; H.H.-H., E.O., K.W., H.B.S., O.T., and H.W. analyzed data; H.H.-H., E.O., K.W., H.B.S., O.T., and H.W. interpreted results of experiments; H.H.-H. and E.O. prepared figures; H.H.-H. and H.W. drafted manuscript; H.H.-H., E.O., O.T., and H.W. edited and revised manuscript; H.H.-H., E.O., K.W., H.B.S., O.T., and H.W. approved final version of manuscript; O.T. and H.W. conception and design of research.

REFERENCES

1. **Aukland K, Tenstad O, Wiig H.** Distribution spaces for hyaluronan and albumin in rat tail tendons. *Am J Physiol Heart Circ Physiol* 281: H1589–H1597, 2001.
2. **Behrendt N.** Human complement component C3: characterization of active C3 S and C3 F, the two common genetic variants. *Mol Immunol* 22: 1005–1008, 1985.
3. **Bernard N, Lombart C, Waks M.** Modification of rat hemopexin properties upon heme binding. *Eur J Biochem* 103: 271–276, 1980.
4. **Bert JL, Pearce RH, Mathieson JM, Warner SJ.** Characterization of collagenous meshworks by volume exclusion of dextrans. *Biochem J* 191: 761–768, 1980.

5. **Bertolatus JA, Abuyousef M, Hunsicker LG.** Glomerular sieving of high molecular weight proteins in proteinuric rats. *Kidney Int* 31: 1257–1266, 1987.

6. **Bokisch VA, Dierich MP, Muller-Eberhard HJ.** Third component of complement (C3): structural properties in relation to functions. *Proc Natl Acad Sci USA* 72: 1989–1993, 1975.

7. **Butcher DT, Alliston T, Weaver VM.** A tense situation: forcing tumour progression. *Nat Rev Cancer* 9: 108–122, 2009.

8. **Choi J, Credit K, Henderson K, Deverkadra R, He Z, Wiig H, Vanpelt H, Flessner MF.** Intraperitoneal immunotherapy for metastatic ovarian carcinoma: resistance of intratumoral collagen to antibody penetration. *Clin Cancer Res* 12: 1906–1912, 2006.

9. **Cortesi L, Rossi E, Della Casa L, Barchetti A, Nicoli A, Piana S, Abrate M, La Sala GB, Federico M, Iannone A.** Protein expression patterns associated with advanced stage ovarian cancer. *Electrophoresis* 32: 1992–2003, 2011.

10. **Gao Y, Yue W, Zhang P, Li L, Xie X, Yuan H, Chen L, Liu D, Yan F, Pei X.** Spindlin1, a novel nuclear protein with a role in the transformation of NIH3T3 cells. *Biochem Biophys Res Commun* 335: 343–350, 2005.

11. **Goel S, Duda DG, Xu L, Munn LL, Boucher Y, Fukumura D, Jain RK.** Normalization of the vasculature for treatment of cancer and other diseases. *Physiol Rev* 91: 1071–1121, 2011.

12. **Gromov P, Gromova I, Olsen CJ, Timmermans-Wielenga V, Talman ML, Serizawa RR, Moreira JM.** Tumor interstitial fluid—a treasure trove of cancer biomarkers. *Biochim Biophys Acta* 1834: 2259–2270, 2013.

13. **Guo J, Yang EC, Desouza L, Diehl G, Rodrigues MJ, Romaschin AD, Colgan TJ, Siu KW.** A strategy for high-resolution protein identification in surface-enhanced laser desorption/ionization mass spectrometry: calgranulin A and chaperonin 10 as protein markers for endometrial carcinoma. *Proteomics* 5: 1953–1966, 2005.

14. **Gyenge CC, Tenstad O, Wiig H.** In vivo determination of steric and electrostatic exclusion of albumin in rat skin and skeletal muscle. *J Physiol* 552: 907–916, 2003.

15. **Hamilton RG.** Human IgG subclass measurements in the clinical laboratory. *Clin Chem* 33: 1707–1725, 1987.

16. **Haslene-Hox H, Oveland E, Berg KC, Kolmannskog O, Woie K, Salvesen HB, Tenstad O, Wiig H.** A new method for isolation of interstitial fluid from human solid tumors applied to proteomic analysis of ovarian carcinoma tissue. *PLoS One* 6: e19217, 2011.

17. **Haslene-Hox H, Oveland E, Woie K, Salvesen HB, Wiig H, Tenstad O.** Increased WD-repeat containing protein 1 in interstitial fluid from ovarian carcinomas shown by comparative proteomic analysis of malignant and healthy gynecological tissue. *Biochim Biophys Acta* 1834: 2347–2359, 2013.

18. **Hiltunen EL, Anttila M, Kultti A, Ropponen K, Penttinen J, Yliskoski M, Kuronen AT, Juhola M, Tammi R, Tammi M, Kosma VM.** Elevated hyaluronan concentration without hyaluronidase activation in malignant epithelial ovarian tumors. *Cancer Res* 62: 6410–6413, 2002.

19. **Jain RK.** The Eugene M. Landis Award Lecture 1996. Delivery of molecular and cellular medicine to solid tumors. *Microcirculation* 4: 1–23, 1997.

20. **Kerr MA.** The structure and function of human IgA. *Biochem J* 271: 285–296, 1990.

21. **Krol A, Maresca J, Dewhirst MW, Yuan F.** Available volume fraction of macromolecules in the extravascular space of a fibrosarcoma: implications for drug delivery. *Cancer Res* 59: 4136–4141, 1999.

22. **Laurent TC.** The interaction between polysaccharides and other macromolecules. The exclusion of molecules from hyaluronic acid gels and solutions. *Biochem J* 93: 106–112, 1964.

23. **Malamud D, Drysdale JW.** Isoelectric points of proteins: a table. *Anal Biochem* 86: 620–647, 1978.

24. **Monteiro RC, Halbwachs-Mecarelli L, Roque-Barreira MC, Noel LH, Berger J, Lesavre P.** Charge and size of mesangial IgA in IgA nephropathy. *Kidney Int* 28: 666–671, 1985.

25. **Netti PA, Berk DA, Swartz MA, Grodzinsky AJ, Jain RK.** Role of extracellular matrix assembly in interstitial transport in solid tumors. *Cancer Res* 60: 2497–2503, 2000.

26. **Norden AG, Lapsley M, Lee PJ, Pusey CD, Scheinman SJ, Tam FW, Thakker RV, Unwin RJ, Wrong O.** Glomerular protein sieving and implications for renal failure in Fanconi syndrome. *Kidney Int* 60: 1885–1892, 2001.

27. **O'Connor SW, Bale WF.** Accessibility of circulating immunoglobulin G to the extravascular compartment of solid rat tumors. *Cancer Res* 44: 3719–3723, 1984.

28. **Oien AH, Justad SR, Tenstad O, Wiig H.** Effects of hydration on steric and electric charge-induced interstitial volume exclusion-a model. *Biophys J* 105: 1276–1284, 2013.

29. **Paiva P, Van Damme MP, Tellbach M, Jones RL, Jobling T, Salamonsen LA.** Expression patterns of hyaluronan, hyaluronan synthases and hyaluronidases indicate a role for hyaluronan in the progression of endometrial cancer. *Gynecol Oncol* 98: 193–202, 2005.

30. **Pan S, Wang R, Zhou X, Corvera J, Kloc M, Sifers R, Gallick GE, Lin SH, Kuang J.** Extracellular Alix regulates integrin-mediated cell adhesions and extracellular matrix assembly. *EMBO J* 27: 2077–2090, 2008.

31. **Pannell R, Johnson D, Travis J.** Isolation and properties of human plasma alpha-1-proteinase inhibitor. *Biochemistry* 13: 5439–5445, 1974.

32. **Pham TV, Piersma SR, Oudgenoeg G, Jimenez CR.** Label-free mass spectrometry-based proteomics for biomarker discovery and validation. *Expert Rev Mol Diagn* 12: 343–359, 2012.

33. **Polanski M, Anderson NL.** A list of candidate cancer biomarkers for targeted proteomics. *Biomark Insights* 1: 1–48, 2007.

34. **Postawski K, Rechberger T, Skorupski P, Jakowicki JA.** Extracellular matrix remodelling within the normal human ovarian capsule. *Eur J Obstet Gynecol Reprod Biol* 67: 173–177, 1996.

35. **Rolny C, Mazzone M, Tugues S, Laoui D, Johansson I, Coulon C, Squadrito ML, Segura I, Li X, Knevels E, Costa S, Vinckier S, Dresselaer T, Akerud P, De Mol M, Salomaki H, Phillipson M, Wyns S, Larsson E, Buysschaert I, Botling J, Himmelreich U, Van Ginderachter JA, De Palma M, Dewerchin M, Claesson-Welsh L, Carmeliet P.** HRG inhibits tumor growth and metastasis by inducing macrophage polarization and vessel normalization through downregulation of PlGF. *Cancer Cell* 19: 31–44, 2011.

36. **Rosen A, Ek K, Aman P.** Agarose isoelectric focusing of native human immunoglobulin M and alpha 2-macroglobulin. *J Immunol Methods* 28: 1–11, 1979.

37. **Sagstad S, Oveland E, Karlsen TV, Haslene-Hox H, Tenstad O, Wiig H.** Age-related changes in rat dermal extracellular matrix composition affect the distribution of plasma proteins as a function of size and charge. *Am J Physiol Heart Circ Physiol*. In press.

38. **Salama I, Malone PS, Mihaimeed F, Jones JL.** A review of the S100 proteins in cancer. *Eur J Surg Oncol* 34: 357–364, 2008.

39. **Schwick HG, Haupt H.** Purified human plasma proteins of unknown function. *Jpn J Med Sci Biol* 34: 299–327, 1981.

40. **Sottrup-Jensen L, Stepanik TM, Kristensen T, Wierzbicki DM, Jones CM, Lonblad PB, Magnusson S, Petersen TE.** Primary structure of human alpha 2-macroglobulin. V. The complete structure. *J Biol Chem* 259: 8318–8327, 1984.

41. **Speeckaert M, Huang G, Delanghe JR, Taes YE.** Biological and clinical aspects of the vitamin D binding protein (Gc-globulin) and its polymorphism. *Clin Chim Acta* 372: 33–42, 2006.

42. **Stewart JJ, White JT, Yan X, Collins S, Drescher CW, Urban ND, Hood L, Lin B.** Proteins associated with Cisplatin resistance in ovarian cancer cells identified by quantitative proteomic technology and integrated with mRNA expression levels. *Mol Cell Proteomics* 5: 433–443, 2006.

43. **Toole BP.** Hyaluronan: from extracellular glue to pericellular cue. *Nat Rev Cancer* 4: 528–539, 2004.

44. **Travis J, Garner D, Bowen J.** Human alpha-1-antichymotrypsin: purification and properties. *Biochemistry* 17: 5647–5651, 1978.

45. **Trovik J, Wik E, Stefansson IM, Marcickiewicz J, Tingulstad S, Staff AC, Njolstad TS, MoMaTec Study G, Vandenput I, Amant F, Akslen LA, Salvesen HB.** Stathmin overexpression identifies high-risk patients and lymph node metastasis in endometrial cancer. *Clin Cancer Res* 17: 3368–3377, 2011.

46. **Voisin SN, Krakovska O, Matta A, DeSouza LV, Romaschin AD, Colgan TJ, Siu KW.** Identification of novel molecular targets for endometrial cancer using a drill-down LC-MS/MS approach with iTRAQ. *PLoS One* 6: e16352, 2011.

47. **Wang TH, Chao A, Tsai CL, Chang CL, Chen SH, Lee YS, Chen JK, Lin YJ, Chang PY, Wang CJ, Chao AS, Chang SD, Chang TC, Lai CH, Wang HS.** Stress-induced phosphoprotein 1 as a secreted biomarker for human ovarian cancer promotes cancer cell proliferation. *Mol Cell Proteomics* 9: 1873–1884, 2010.

48. **Wiig H, Aukland K, Tenstad O.** Isolation of interstitial fluid from rat mammary tumors by a centrifugation method. *Am J Physiol Heart Circ Physiol* 284: H416–H424, 2003.

49. **Wiig H, Gyenge CC, Tenstad O.** The interstitial distribution of macro-molecules in rat tumours is influenced by the negatively charged matrix components. *J Physiol* 567: 557–567, 2005.

50. **Wiig H, Kolmannskog O, Tenstad O, Bert JL.** Effect of charge on interstitial distribution of albumin in rat dermis in vitro. *J Physiol* 550: 505–514, 2003.

51. **Wiig H, Swartz MA.** Interstitial fluid and lymph formation and transport: physiological regulation and roles in inflammation and cancer. *Physiol Rev* 92: 1005–1060, 2012.

52. **Woessner JF.** The determination of hydroxyproline in tissue and protein samples containing small proportions of this imino acid. *Arch Biochem Biophys* 93: 440–447, 1961.